



Application of Micro Structured Fiber Sensor in the Field of Temperature Detection

Tianyu Yang^a, Tao Shen*^{a,b,c}, Yue Feng^{a,b}, Xin Liu^{b,c}

^aHeilongjiang Province Key Laboratory of Laser Spectroscopy Technology and Application, Harbin University of Science and Technology, Harbin 150080, China.

^bKey Laboratory of Engineering Dielectrics and Its Application, Ministry of Education, Harbin University of Science and Technology, Harbin, 150080, China.

^cHeilongjiang Provincial Key Laboratory of Quantum Control, Harbin University of Science and Technology, Harbin 150080, China.

*corresponding author

e-mail: taoshenchina@163.com

Abstract—A fiber temperature sensor based on no core fiber-few mode fiber-no core fiber (NCF-FMF-NCF) is proposed. It consists of two segments of NCF and a segment of FMF, with the NCF fused at both ends of the FMF. Meanwhile, the lengths of the NCF and FMF were optimized by simulation simulations and experimental validation. The results show that the sensor has a high sensitivity to the external refractive index (RI) changes, and enables a wide range of ambient temperature measurement. A sensitivity of 0.09445nm/°C was obtained in a temperature range of 25-70°C. The sensor has the advantages of high stability, good linear fit and simple structure.

Keywords- Temperature sensor; Optical fiber sensing; Intermodal interference; NCF; FMF

I. INTRODUCTION

Fiber optic temperature sensor has been widely used in the field of temperature measurement due to its good flexibility, resistance to electromagnetic interference and high sensitivity [1-3]. There are many kinds of optical fiber temperature sensors, and their sensing mechanism is not the same. The common optical fiber temperature sensors mainly include interference type, grating type and surface plasma resonance (SPR) type of optical fiber temperature sensors [4-6]. The sensing principles of these three types of optical fiber temperature sensors are quite different, and the temperature measurement performance and the use environment are also quite different. Temperature sensors based on interferometric, grating, and SPR types have been proposed. Lei et al. have proposed a high-temperature optical fiber sensor with a multimode fiber-fine core fiber-multimode fiber structure based on the principle of MZI interference. The measured temperature sensitivity was 0.150nm/°C. However, multimode optical fibers produce many high-mode modes, which are very sensitive to the external environment, and do not use spectral control and stability [7]. Subsequently, Luo et al. proposed a D-type fiber temperature sensor based on graphene

(Gr) and polydiD-methyl siloxane (PDMS) materials [8]. The effect of graphene with different layers on sensor sensitivity was explored and showed that the best graphene layers were 4, with a sensitivity of 1.56nm/°C. However, the preparation process of this sensor has a high cost and complexity. Zhao et al. have developed an optical fiber temperature sensor based on a 45° inclined fiber optic polarator (TFBG-PIF-TS) based on the principle of fiber optic grating [9]. The measurement accuracy reached $\pm 0.1^\circ\text{C}$. However, the cost of TFBG is very high, and it cannot be widely used. Therefore, these sensors generally have problems such as low sensitivity, very high production cost and more complex production process.

To improve the sensitivity and reduce the manufacturing difficulty, we propose an optical fiber temperature sensor based on the NCF-FMF-NCF structure. The structure has the advantages of high sensitivity, simple manufacture and low cost. Moreover, its properties have been validated in experiments and simulations. The sensitivity has reached 0.09445nm/°C in the temperature range of 25-70°C.

II. STRUCTURE DESIGN AND PRINCIPLE

A. Sensor Preparation

As shown in Fig. 1, the structure of the sensor is easy to implement, with low production cost and simple structure. First, the first step is to use the optical fiber fusion machine splicing. Second, the second step will splice the FMF with NCF1. Finally, the third step has fused the previously spliced parts with the NCF2 and SMF to form the SMF-NCF1-FMF-NCF2-SMF structure. The lengths of its NCF1, NCF2, and FMF have been discussed in the simulation analysis below, resulting in an optimal length with an NCF of 15mm and an FMF of 20mm.

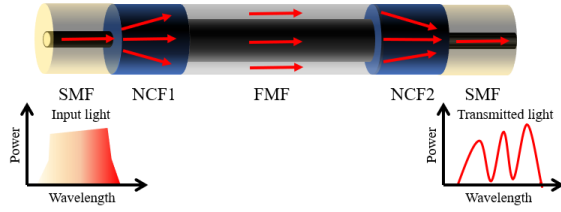


Fig. 1. Structure of SMF-NCF1-FMF-NCF2-SMF sensor unit.

B. Sensing principle

Since SMF and NCF are unbiased fused. When light is transmitted to NCF1 through SMF, only the higher-order eigenmode LP_{0m} is excited in NCF because the input field has angular symmetry and the fiber has a central symmetric structure. After passing through the FMF, the excited higher-order mode is transmitted simultaneously in the cladding layer and in the fiber core base mode. The presence of a phase difference recoupled to the inner SMF core when different modes of light propagate to the melting junction of the NCF2 and the SMF causes interference in different modes of light. The intensity of the interference light can be expressed as [10]:

$$I = I_1 + I_2 + 2\sqrt{I_1 I_2} \cos \varphi_0$$

I_1 is the optical intensity of the fiber core base mode, and I_2 is the optical intensity of the higher-order mode of the envelope. Furthermore, the phase difference φ_0 is expressed as follows:

$$\varphi_0 = \frac{2\pi\Delta n_{eff}L}{\lambda} = \frac{2\pi(n_{core} - n_{cl})L}{\lambda}$$

Δn_{eff} is the difference between the effective incidence of the fiber core mode and the effective refractive index of the envelope, n_{core} is the effective refractive index of the fiber core mode, n_{cl} is the effective refractive index of the envelope mode, and L is the interference length. Furthermore, when $\varphi_0 = (2m+1)\pi$, m is an integer, then the resonance wavelength of the m -order interference stripe is specifically expressed as:

$$\lambda_m = \frac{2\pi\Delta n_{eff}L}{(2m+1)\pi} = \frac{2\Delta n_{eff}L}{(2m+1)}$$

As can be seen from the equation, the resonance wavelength λ_m drift is affected by Δn_{eff} and L . When L is fixed, the drift of the resonance wavelength varies with Δn_{eff} . Therefore, the refractive index change of the external environment is measured by detecting the drift amount of the resonance wavelength. The *FSR* (free spectral range) can be expressed as:

$$FSR \approx \frac{\lambda^2}{\Delta n_{eff}L} = \frac{\lambda^2}{\Delta n_{eff}(L_1+L_2+L_3)}$$

Where, L_1 , L_2 , and L_3 are the interference lengths of NCF1, FMF, and NCF2, respectively. The *FSR* is obtained as inversely proportional to the length of the sensing structure. Let the light field input from the SMF be $E(r, 0)$, and the m -order mode in the NCF be $F_m(r)$, at the input SMF and NCF1 connection[11]:

$$E(r, 0) = \sum_{m=1}^N c_m F_m(r)$$

In the equation: N is the total number of modes present in the NCF, and c_m is the light field excitation coefficient of the m -order mode. The c_m can be expressed as:

$$c_m = \frac{\int_0^\infty E(r, 0)F_m(r)rdr}{\int_0^\infty F_m(r)F_m(r)rdr}$$

When the light travels a Z distance, the light field of the NCF core portion can be expressed as:

$$E(r, z) = \sum_{m=1}^M c_m F_m(r) \exp(i\beta_m z)$$

The β_m is the longitudinal propagation constant of the m -order pattern. At the melting point of NCF1 and FMF, when the light of some m -order mode enters the fiber core of the FMF and coupled to the envelope of the FMF, then the coupling coefficient d_n of its n -order envelope mode can be expressed as:

$$d_n = \frac{\int_0^\infty \sum_{m=1}^M c_m F_m(r) \exp(i\beta_m L_N) f_n(r) r dr}{\int_0^\infty f_n(r) f_n(r) r dr}$$

L_N is the NCF length, $E(r, L_N)$ is the field distribution of the transmission L_N distance, and $f_n(r)$ is the field distribution of the FMF. It is concluded that the excitation of the n -order mode in the FMF depends on the phase of the m -order mode conduction in the NCF. Thus, the field distribution in the FMF is affected by the NCF1 length modulation. And at NCF2, there is mode interference between the base mode of the FMF and the higher order mode.

As shown in Fig. 2 (a), the light field distribution in the NCF simulates the X axis represents the radius direction of the fiber, and the Z axis represents the fiber longitudinal direction, that is, the optical propagation distance. With the different transmission length of the light signal in the NCF, the light field distribution will appear periodically reproduced phenomenon, which is the image effect. Moreover, the energy of the light field at the self-image is the same as the incident light field, so the light field here is the most intense, and the greater the light energy coupled to the output SMF will be.

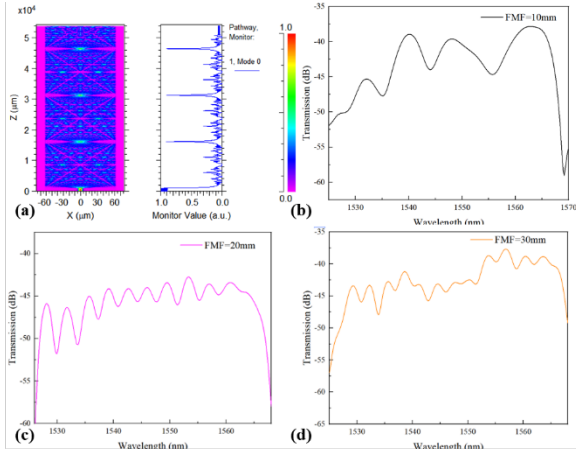


Fig. 2. (a) Plot of the light field distribution in the NCF; (b) Interference spectrum of the sensor at FMF=10mm; (c) Interference spectrum of the sensor at FMF=20mm; (d) Interference spectrum of the sensor at FMF=30mm.

To explore the optimal transmission spectrum of the NCF1-FMF-NCF2 fiber structure, we first determine the optimal length of the NCF by the simulation analysis above, with the autoenographic points at 15mm, 30mm, 45mm. Considering the integration of the fiber structure and the FSR effect, an NCF of length 15mm was selected for the study. As shown in Fig. 2 (b-d), the influence of FMF of different lengths on the transmission spectrum of the sensor was explored. The FMF lengths were 10 mm, 20 mm and 30 mm, respectively, which showed that the FMF interference effect of 10 mm was optimal

C. Experimental equipment

An experimental setup for temperature sensing, as shown in Fig. 3. It includes an ASE light source, a temperature sensor, and a spectrum analyzer (OSA: AQ6370D). The central wavelength of the ASE source is 1550 nm, with a wavelength range ranging from 1523 nm to 1573 nm. The OSA has a resolution of 0.02 nm and a detection range ranging from 600 nm to 1700 nm. The temperature sensor consists of the designed NCF1-FMF-NCF2 fiber structure. Place the sensor in the temperature control box for the temperature range of 25-70°C, and change the ambient temperature inside the temperature box. During the measurement process, the optical fiber sensor is necessary to be fixed to the glass slide to ensure that the structure remains stable during the measurement process.

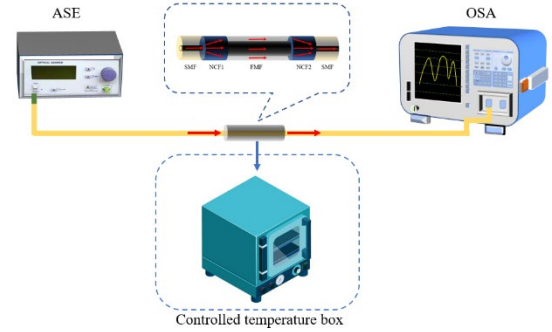


Fig. 3. Diagram of temperature sensing experiment device.

D. Experiments and Results analysis

Fig. 4(a) shows the interference spectrum of NCF1-FMF-NCF2. Temperature range is 25-75°C, step length is 5°C, each increase of 5°C wait for 3min, when the interference spectrum stability data recording.

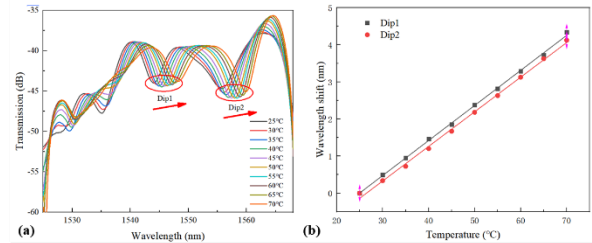


Fig.4 (a) The linear dependence of the interference spectrum with temperature; (b) Linear fit of the interference spectral shift to the temperature change.

As shown in Fig. 4(b), when the temperature increases from 25°C to 70°C, the interference spectrum is shifted (redshift) toward the long wavelength, Dip1 is 0.09445nm/°C, Dip2 is 0.09328nm/°C, and the linear fitting coefficient reaches 0.99916 and 0.99792, respectively.

III. CONCLUSIONS

An optical fiber temperature sensor based on the NCF-FMF-NCF structure is presented. The NCF-FMF-NCF sensing unit is prepared by fusion method, combining mode interference principle and evanescent field theory for high sensitivity detection under evanescent field theory. The experimental results show that the highest sensor sensitivity reached 0.09445nm/°C and the linearity reached 0.99916 in the temperature variation range of 25-70°C. The sensor has good stability, high sensitivity, good linearity, low cost, and simple manufacturing process. It has a good application prospect in the field of temperature monitoring.

ACKNOWLEDGMENT

The research was supported by the National Natural Science Foundation of China (52102164)

REFERENCES

- [1] Cai L, Liu Y, Hu S, et al. Optical fiber temperature sensor based on modal interference in multimode fiber lengthened by a short segment of polydimethylsiloxane[J]. *Microwave and Optical Technology Letters*, 2019, 61(6): 1656-1660.
- [2] Zhang C, Ning T, Zheng J, et al. Miniature optical fiber temperature sensor based on FMF-SCF structure[J]. *Optical Fiber Technology*, 2018, 41: 217-221.
- [3] Chu R, Guan C, Bo Y, et al. Temperature sensor in suspended core hollow fiber covered with reduced graphene oxide[J]. *IEEE Photonics Technology Letters*, 2019, 31(7): 553-556.
- [4] Ma J, Wu S, Cheng H, et al. Sensitivity-enhanced temperature sensor based on encapsulated S-taper fiber Modal interferometer[J]. *Optics & Laser Technology*, 2021, 139: 106933.
- [5] Tong R, Zhao Y, Hu H, et al. Large measurement range and high sensitivity temperature sensor with FBG cascaded Mach-Zehnder interferometer[J]. *Optics & Laser Technology*, 2020, 125: 106034.
- [6] Laarossi I, Quintela-Incera M Á, López-Higuera J M. Comparative experimental study of a high-temperature raman-based distributed optical fiber sensor with different special fibers[J]. *Sensors*, 2019, 19(3): 574.
- [7] X Q Lei, Y Feng, X P Dong. High-temperature sensor based on a special thin-diameter fiber, *Optics Communications*, 2020, vol. 463: pp. 0030-4018.
- [8] Luo J, Liu G S, Zhou W, et al. A graphene-PDMS hybrid overcoating enhanced fiber plasmonic temperature sensor with high sensitivity and fast response[J]. *Journal of Materials Chemistry C*, 2020, 8(37): 12893-12901.
- [9] Zhao J, Wang H, Sun X. Study on the performance of polarization maintaining fiber temperature sensor based on tilted fiber grating[J]. *Measurement*, 2021, 168: 108421.
- [10] Zhao F, Xiao D, Lin W, et al. Sensitivity Enhanced Rrefractive Index Sensor with In-Line Fiber Mach-Zehnder Interferometer Based on Double-Peanut and Er-Doped Fiber Taper Structure[J]. *Journal of Lightwave Technology*, 2022, 40(1): 245-251.
- [11] Zhang J, Tong Z, Zhang W, et al. Research on NCF-PCF-NCF Structure Interference Characteristic for Temperature and Relative Humidity Measurement[J]. *IEEE Photonics Journal*, 2021, 13(4): 1-5.